Ferromagnetic Artifacts in MRI: Minimization of Motion Effects in Long T_R Acquisitions

Eric Aboussouan, *Student Member IEEE*, and Sylvain Martel*, *Member IEEE*

NanoRobotics Laboratory, Department of Computer Engineering and Institute of Biomedical Engineering,
École Polytechnique de Montréal (EPM), Campus of the Université de Montréal, Montréal (Québec) Canada

*E-mail: sylvain.martel@polymtl.ca URL: www.nano.polymtl.ca

***Abstract*— A feasibility study is under way for a multiplexed tracking/imaging/propulsion sequence to control a ferromagnetic microdevice in the human vasculature. Ferromagnetic artefact motion can be problematic for the acquired images but we show that when the phase encoding direction is made to match the main direction of motion of the device, the acquisition of planes distant of 3.4 cm of the ferromagnetic bead used show acceptable distortions and signal loss even when the bead incurs significant motion during acquisition. At approximately 6.4 cm, no distortion or signal loss is observed. These results suggest that slow breathing motion can be measured and/or gated using the undistorted parts of the images.**

***Index Terms*— Ferromagnetic artifacts, motion, MRI, microdevice, sequence multiplexing**

I. Introduction

The MR-Sub (Magnetic Resonance Submarine) project of the NanoRobotics Laboratory of the École Polytechnique of Montreal consists in an untethered endovascular microdevice that is tracked [1], propelled [2] and controlled using a commercial Magnetic Resonance Imaging (MRI) apparatus. The preliminary results suggest that such a device can be developed to navigate in the human blood system in order to perform specific medical tasks in hard to reach regions of the vasculature.

Tracking and propulsion sequences have already been integrated in order to control the device between the waypoints of a pre-acquired roadmap. This roadmap however is subjected to spatial deformations due to body motion (such as respiration-induced movements). This body motion could be evaluated by different means, including external stereotactic tracking systems. Although some of these systems can be made MR-compatible, their use in this context would be problematic. Indeed, they would forbid the use of a body array antenna which would hinder the line of sight of the system. Moreover, the use of such a system would suffer from additional complications and uncertainties imputable to the registration of the different coordinates systems to the MRI coordinates.

A preliminary study is currently underway to assess the possibility of using portions of intra-operational MRI image acquisitions to track internal or external fiducials [4,5], thus simplifying significantly the required setup and avoiding the previously discussed caveats.

The core of the micro-device is made of a ferromagnetic particle, allowing us to propel it using MRI gradients. The use of ferromagnetic material, however, creates distortion of the surrounding magnetic field which gives rise to errors during the eventual image encoding process. As a result, the acquired images can suffer susceptibility artifacts, seen as both geometric and intensity distortions. Moreover, the significant motion of the ferromagnetic particle that can occur during those image acquisitions has not yet, at our knowledge, been addressed in the literature.

The hypothesis validated in this paper is that there are planes distanced by a couple of centimeters from the bead on which the ferromagnetic image distortions are negligible. The signal void however cannot always be considered negligible, especially when the bead is moving. Nonetheless, we demonstrate here that by choosing a phase encoding direction parallel to the direction of the bead motion, the signal loss region can be spatially limited and kept inside a deterministic region. The unaffected regions will then be usable for body motion measurements and/or gating as stated previously.

II. Theory

A. Tracking/Propulsion/Imaging multiplexing

In order to acquire images without loosing too much of the temporal resolution of the tracking, it is imperative to use appropriate multiplexing. The image acquisitions would thus have to be partitioned in groups of K-space lines readings interleaved with tracking and propulsion sequence blocks. This, however, would result in long T_R imaging sequences. Because the motion of the body due to respiration is relatively slow, it is thought that an imaging frequency in the order of a second would be sufficient for this measurement. The motion of the ferromagnetic device, however, could be significant during such an image acquisition. The effect of such motion will be addressed later on.

B. Distortions due to static ferromagnetic particles

Susceptibility artifacts in MRI have been studied thoroughly in the past [6-8] The severity of such image

aberrations depends upon the distortion source's magnetic properties, shape and orientation, as well as certain imaging parameters and the choice of sequence itself. Because of the severe inhomogeneity generated by the presence of the ferromagnetic in the imaged volume, a distortion in the selected slice may occur. This plane warp is due to spins outside the desired slice responding to the frequency of the RF pulse because of the presence of a perturbing field. Errors in the frequency and phase encoding directions may also occur and their magnitude would vary with the sequence and parameter used, as stated earlier. For planes far enough of the source of inhomogeneity, the distortions and signal loss can be considered negligible. For closer planes however, those phenomenon can be important in certain parts of the image.

For the remaining of this theoretical section, we will assume that the only image artefact is a loss of signal in the surroundings of the bead. This simplification will be justified experimentally but suffice to say here that the signal loss is more damageable than small distortions because it adds high contrast regions that can be hard to distinguish from actual features. It is also worthwhile to notice that this approximation will be closer to reality for gradient-echo than for spin echo sequences. Indeed, the gradient echo sequence does not refocus the dephasing due to ferromagnetic gradient. A position dependant phase is added in the region of inhomogeneity which disturbs the echo and leads to a black (or white, if the interference is constructive) area which will be referred as signal loss in the rest of this text. Note also that although spin echo sequences display less signal loss than gradient echo sequences, the latter sequence type was chosen here because it allows the use of smaller flip angles during imaging. This will reduce the effect of the imaging sequence on the positioning because of the minimized remanent magnetization.

C. Analytical model of the signal loss motion during a long-T_R MRI acquisition

Here, it is important to look at the effect on the MR-image when the ferromagnetic bead moves significantly during its acquisition. The centre of the hole will be described parametrically by $h_x(t)$ and $h_y(t)$ in that plane, where x corresponds to the readout direction and y to the phase-encoding direction. Starting from the simple and acceptable assumptions previously stated, we can prove that the resulting image will remain undistorted for some definite regions of the image.

Let us define $H(x, y) \in \{0,1\}$ the binary mask representing a hole (signal loss) centered at the origin. An image $I_s(x,y)$ taken with a steady hole centered in (h_x, h_y) can thus be written:

$$I_s(x,y) = I_0(x,y) .* (1-H(x, y) \otimes\otimes \delta(h_x, h_y)) \qquad (1)$$

where I_0 is the untouched image, $\delta(h_x, h_y)$ represents a Kronecker delta centered in (h_x, h_y), '$\otimes\otimes$' represents a 2-D convolution and '.*' denotes the element-by-element multiplication. Taking the Discrete Fourier Transform (DFT) F_h of I_h, we get:

$$\begin{aligned} F_s(u,v) &= \Im(I_s(u,v)) \\ &= F_0(u,v) - F_0(u,v) \otimes\otimes \left(F_h(u,v) .* e^{-j2\pi(h_x u + h_y v)} \right) \end{aligned} \qquad (2)$$

Next, the effect of the movement on a long T_R acquisition must be examined. Because T_E is short compared to T_R, we can assume that no motion occurs between the acquisitions of a single K-space line, that is to say:

$$h_x(t) = h_x(t+T_E+T_s/2) \,,\; h_y(t) = h_y(t+T_E+T_s/2) \qquad (3)$$

where Ts is the sampling time. Between each K-space line acquisition, however, the bead will have time to move significantly:

$$h_x(t) \neq h_x(t+T_R) \,,\; h_y(t) \neq h_y(t+T_R) \qquad (4)$$

The resulting K-space acquisition F_m can be modeled by mosaicing the readout lines of F_h:

$$\begin{aligned} F_m(u,v) &= \begin{bmatrix} F_s(u,v_0) \\ \vdots \\ F_s(u,v_{max}) \end{bmatrix} \\ &= F_0(u,v) - F_0(u,v) \otimes\otimes \left(F_h(u,v) .* M(u,v) \right) \end{aligned} \qquad (5)$$

with:

$$M(u,v) \equiv \begin{bmatrix} e^{-j2\pi(h_x(t_0)u + h_y(t_0)v_0)} \\ \vdots \\ e^{-j2\pi(h_x(t_{end})u + h_y(t_{end})v_{max})} \end{bmatrix}, \qquad (6)$$

where u and v are the readout and phase-encoding direction respectively, t_0 is the time when the first phase line (v_0) is acquired and t_{max} the time when the last phase line (v_{max}) is acquired.

Taking the inverse DFT Im(x,y) of Fm(u,v) we get the expression:

$$\begin{aligned} I_m(x,y) &= \Im^{-1}(F_m(u,v)) \\ &= I_0(x,y) - I_0(x,y) .* \left(H(x,y) ** \Im^{-1}(M(u,v)) \right) \end{aligned} \qquad (7)$$

That is to say that the distortion will be a convolution of the hole H(x,y) with a distribution $\Im^{-1}(M(u,v))$.

The characteristics of this distribution can be studied:

$$\Im^{-1}(M(u,v)) = \sum_{u=0}^{M-1} \sum_{v=0}^{N-1} \left(\begin{bmatrix} e^{-j2\pi\left(h_x(t_0)\frac{u}{M} + h_y(t_0)\frac{0}{N}\right)} \\ \vdots \\ e^{-j2\pi\left(h_x(t_{end})\frac{u}{M} + h_y(t_{end})\frac{N-1}{N}\right)} \end{bmatrix} .* e^{j2\pi\left(\frac{ux}{M} + \frac{vy}{N}\right)} \right). \qquad (8)$$

By separating the two inverse DFTs, it can be shown that this is equivalent to:

$$\Im^{-1}(M(u,v)) =$$

$$\begin{bmatrix} \delta(\text{x-h}_x(\text{t}_0)) \\ \vdots \\ \delta(\text{x-h}_x(\text{t}_{end})) \end{bmatrix} .* \sum_{v=0}^{N-1} \left(\begin{bmatrix} e^{\text{j}2\pi\frac{0}{\text{N}}(\text{y-h}_y(\text{t}_0))} \\ \vdots \\ e^{\text{j}2\pi\frac{\text{N-1}}{\text{N}}(\text{y-h}_y(\text{t}_{end}))} \end{bmatrix} \times [1 \quad \cdots \quad 1] \right) \qquad (9)$$

where × represents the outer product of 2 vectors. Since $\delta(x-x_0)=0$, $\forall x \neq x0$, we show that:

$$\Im^{-1}(M(u,v)) = 0 \text{ for } (x < h_{xmin}) \cup (x > h_{xmax}). \qquad (10)$$

The distortion will thus be limited to a region inside a band ($h_{xmin} - R_L < x < h_{xmax} + R_R$), where R_L and R_R are respectively the extent of the hole H(x,y) to the left and to the right of the origin: R_L = Min(x): ∃y, H(x,y) ≠ 0, R_R = Max(x): ∃y, H(x,y) ≠ 0.

From this result we can determine an optimal encoding scheme to minimize the movement distortion. Suppose now that x and y constitute an arbitrary system of coordinates in the slice plane. By rotating the phase encoding direction y' to match it with the main component of the expected motion, we optimally reduce the extent of the blurred region in the new readout direction x':

$$\begin{bmatrix} x' \\ y' \end{bmatrix} = \frac{1}{\sqrt{\Delta h_x^2 + \Delta h_y^2}} \begin{bmatrix} \Delta h_y & -\Delta h_x \\ \Delta h_x & \Delta h_y \end{bmatrix} \begin{bmatrix} x \\ y \end{bmatrix} \qquad (11)$$

where Δhx (Δhy) is the total expected motion in the x (y) direction. Note that since this equation does not time independent, this result will remain valid no matter which strategy we choose to fill and/or partition the K-space (sequentially, low frequencies last, etc.)

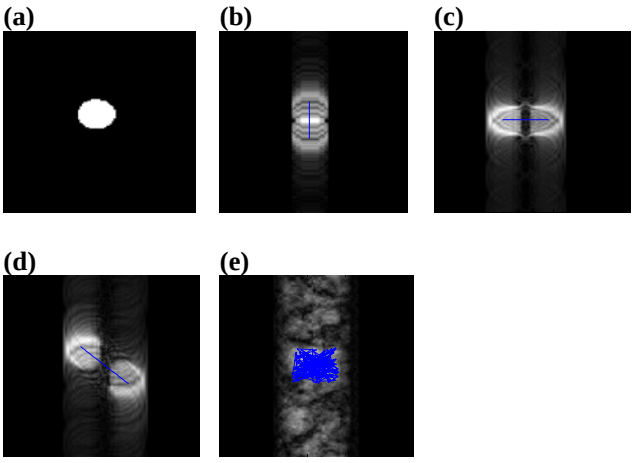

Fig. 1: Computer simulations of the mathematical model for a bead a) immobile b) in motion parallel to the phase-encoding direction c) in motion parallel to the phase-encoding direction e) motion in diagonal motion f) in random motion. A white region represents a signal loss.

For a bead motion having a component perpendicular to the imaged plane, the same analysis applies, where the size of the static signal loss area used is the worst one, that is, the one when the bead was closer to the plane. This would give a worst case scenario of the signal loss encountered.

III. Method

A. Computer simulations

Computer simulations were run to evaluate empirically the validity of the mathematical model described in Sect II.C. A circular region similar to the one in Fig. 1a was used to simulate a signal loss due to a ferromagnetic bead placed at a given distance of the imaged plane. The horizontal lines correspond to the readout direction and the columns to the phase-encoding direction. This signal loss pattern was displaced vertically, horizontally, diagonally and in a random motion. To mimic the long T_R acquisitions, one horizontal line of the 2D DFT was kept for each position of the bead, starting from the top and going towards the bottom. The images obtained for the different motion patterns described previously are reconstructed by inverse DFT and are shown in Fig. 1a–e.

The distortion of the black background is seen to be spread vertically from top to bottom but spans only from the leftmost to the rightmost position of the signal loss during its displacement.

B. MRI experiments

Several images were taken for planes at different distances of a ferromagnetic bead during up-and-down motion. The experiments were conduced for phase encoding direction parallel and perpendicular to the motion. The ferromagnetic core was a chrome-steel ball of diameter 1.5 mm with saturation magnetization of 1.8 T. It was entirely saturated when placed in the 1.5 T static field of the Siemens Magnetom MRI system used. The custom phantom used (Fig. 2) is composed of a set of evenly spaced grids (15.0 mm × 15.0 mm × 12.4 mm). It was precisely machined to measure inhomogeneities of the magnetic field.

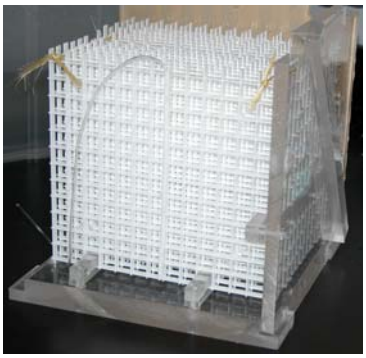

Fig. 2: MRI phantom used

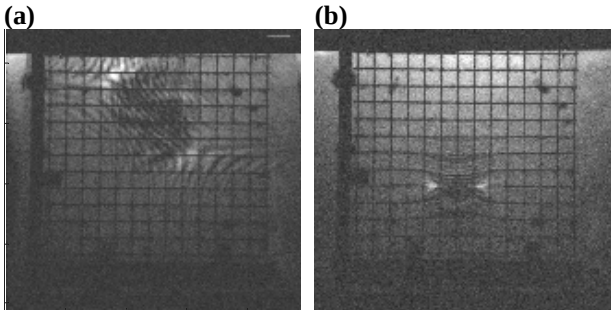

Fig. 3: Image acquisitions during up-and-down motion of a bead placed at 34 mm of the plane with bead motion a) perpendicular to phase encoding direction b) parallel to phase encoding direction.

IV. Experimental Results

The Fig. 3 and Fig. 4 display the experimental results for plane-bead distances of 34 mm and 64 mm respectively. Images were median filtered to remove 'salt and pepper' noise. The body array antenna was placed on the top of the phantom which explains why the top of the images appear brighter. The small dark spots on the grid are due to air bubbles and are irrelevant to our analysis. The simulated maximum field inhomogeneity in the plane at 34 mm and 64 mm was 2.5 μT and 1.0 μT respectively. Fig. 3a shows an acquisition during which the bead was moving in a direction perpendicular to the phase encoding direction. Although the grid shows very little distortion, the image displays widely spread black and white bands similarly to the simulation results. Fig. 3b, however, displays a signal loss concentrated in a small region as predicted earlier. The distorted area on this image is also seen to be limited to a small area close to the signal loss, which corroborates the hypothesis that it can be ignored in the theoretical development. Those results indicate that at relatively close range of the ferromagnetic bead, portions of the image can still be used if the phase encoding direction is judiciously chosen. Further away, all effects of the distortion are eliminated no matter which phase encoding direction is chosen, as depicted in Fig. 4.

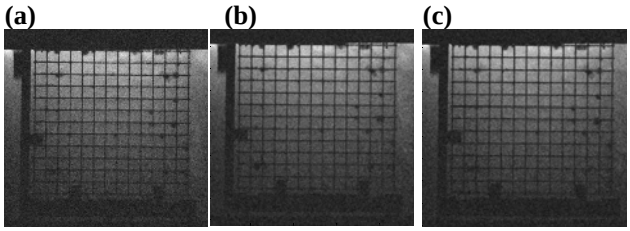

Fig. 4: Image acquisitions with no visible distortions. a) and b) had a bead placed at 34 mm of the plane with bead motion a) parallel to phase encoding direction b) perpendicular to phase encoding direction c) had no bead present during acquisition.

V. Conclusion

A mathematical model has been developed to evaluate the effect of motion on the patterns of signal loss due to ferromagnetic inhomogeneity. The model suggests that the spatial extent of the usable portions of the images can be maximized by matching the direction of motion with the phase-encoding direction. The minimally distorted parts of the images could then be used to gather information on the patient position and/or orientation as well as respiration.

In planes distant by 6.4 cm of the bead, no ferromagnetic distortion or signal loss was observed with the bead used. On closer planes (approximately 3.4 cm from the bead), ferromagnetic distortion was found to be insignificant for our applications. The signal loss, however, is found to add high contrasts bands that can be hard to distinguish from actual features. By rotating the phase encoding direction to follow the main direction of motion of the bead, it was shown that those signal loss areas can be contained in a small, deterministic area as predicted by the model.

ACKNOWLEDGMENT

This project is supported in part by a Canada Research Chair (CRC) in Micro/Nanosystem Development, Fabrication and Validation, the Canada Foundation for Innovation (CFI), the National Sciences and Engineering Research Council of Canada (NSERC), and the Government of Québec. The authors acknowledge the help of Ouajdi Felfoul, Jean-Baptiste Mathieu and Michelle Baryliuk as well as the other team members of the MR-Sub project.

REFERENCES

[1] E. Aboussouan, O. Felfoul, J.-B. Mathieu, and S. Martel, "Real-time projection based technique for tracking ferromagnetic devices", *ISMRM*, 2006 (to be published).

[2] J.B. Mathieu, G. Beaudoin, and S. Martel, "Method of propulsion of a ferromagnetic core in the cardiovascular system through magnetic gradients generated by an MRI system," *IEEE Transactions on Biomedical Engineering*, vol. 53, no. 2, pp. 292-299, 2006.

[4] A. Schweikard, H. Shiomi,, and J. Adler, "Respiration tracking in radiosurgery," *Med. Phys.*, vol. 31, no. 10, pp. 2738-41, Oct. 2004

[5] N. Koch, H. Liu, G. Starkschall, M. Jacobson, K. Forster, Z. Liao, R. Komaki, and C. W. Stevens, "Evaluation of internal lung motion for respiratory-gated radiotherapy using MRI: Part I - Correlating internal lung motion with skin fiducial motion," *International Journal of Radiation Oncology Biology Physics*, vol. 60, no. 5, pp. 1459-1472, 2004

[6] J. F. Schenck, "The role of magnetic susceptibility in magnetic resonance imaging: MRI magnetic compatibility of the first and second kinds", *Medical Physics*, vol. 23, pp. 815-850, 1996.

[7] C.J.G. Bakker, R. Bhagwandien, M. A. Moerland, and L. M. P. Ramos, "Simulation of susceptibility artifacts in 2D and 3D Fourier transform spin-echo and gradient-echo magnetic resonance imaging", *Magn. Res. Imag.*, vol.12, no.5, pp.767-74, 1994.

[8] A. Ericsson, A. Hemmingsson, B. Jung, and G. O. Sperber, "Calculation of MRI artifacts caused by static field disturbances," *Physics in Medicine and Biology*, vol. 33, no. 10, pp. 1103-12, 1988.